INVESTIGATION OF SITE RESPONSE IN KATHMANDU VALLEY USING AFTERSHOCK DATA OF THE 2015 GORKHA EARTHQUAKE, NEPAL

Naresh MAHARJAN[*] **Supervisor: Toshiaki YOKOI**[**]
MEE17704 **Takumi HAYASHIDA**[**]

ABSTRACT

We used 16 aftershock recordings of the 2015 Gorkha earthquake (Mw 7.8) at three temporary stations inside the Kathmandu Valley to derive earthquake H/V spectral ratios (EHVSRs) and compare those with microtremor H/V spectral ratios (MHVSRs) at same stations. The predominant frequency peaks of EHVSRs and MHVSRs are comparable at three continuous observation stations with three-component accelerometers; NAKRM (0.6 Hz), NANST (0.32 Hz) and NABKT (2.2 Hz) suggesting that accelerometers can sometimes be used to investigate response of the deep sedimentary basin. We also derived MHVSRs using microtremor data at 11 temporary sites inside the Kathmandu Valley to obtain dominant frequencies. Next we estimated the thickness of sedimentary layer by calculating theoretical H/V ratio with simplified four-layered velocity model and compared them with the derived MHVSRs. The estimations indicate that the thickness of sedimentary layer ranges from 42 to 700 m. We also investigated amplification and attenuation property of S-waves inside Kathmandu using three earthquakes; one teleseismic event and two aftershocks of the 2015 Gorkha earthquake. Observed data clearly showed that the basin amplifies ground motion in the low frequency range (0.1 – 1.0 Hz), while high-frequency ground motion (>1 Hz) do not rapidly decay in the Kathmandu Valley.

Keywords: H/V spectral ratio, Site Amplification, Kathmandu Valley, Microtremor, Gorkha Earthquake aftershocks.

1. INTRODUCTION

The Kathmandu Valley is an intermountain basin located in the Central Nepal, Lesser Himalaya. The basin was a paleo-lake and sediments were deposited from the surrounding mountains and have estimated the thickness of sedimentary layer more than 600 m (Moribayashi and Mauro, 1980). It has an EW elongation of 30 km and NS elongation of 25 km with an average altitude of 1340 m. The Gorkha earthquake (Mw 7.8) occurred on April 25, 2015 took 8979 lives and destroyed 610720 houses in whole Nepal (1,739 lost their lives and about 13% of buildings were completely damaged in the Kathmandu Valley). Five strong-motion sensors were deployed inside Kathmandu Valley before the mainshock data and the data showed the long-period ground motion with dominant period at 4 to 5 s (Bhattarai et al., 2015; Takai et al., 2016; Dhakal et al., 2016). Also some researchers estimated 1D S-wave velocity structure models using aftershock data inside Kathmandu Valley and found clear velocity contrast between sedimentary layer and bed rock.

2. METHODOLOGY

[*]Department of Mines & Geology (DMG), Nepal.
[**] International Institute of Seismology and Earthquake Engineering, Building Research Institute, Japan.

2.1. H/V Spectral Ratios

Microtremor is defined as a very weak motion generated by natural phenomena and human activities. Kanai and Tanaka (1954) discovered that the dominant frequency of microtremor corresponds to the resonant frequency of subsurface soil. Later, Nakamura (1988) proposed that MHVSR could be a responsible tool to estimate site amplification factor. The similarity and relationship between MHVSR and EHVSR have been discussed over a long period of time. In this study, we used both earthquake and microtremor recordings to identify dominant frequencies of observation sites in Kathmandu Valley and compare EHVSRs and MHVSRs at the same sites. The spectral ratios are derived as follows.

$$\left(\frac{H}{V}\right)_S(f) = \sqrt{\frac{NS^2(f) + EW^2(f)}{UD^2(f)}} \quad , \tag{1}$$

where NS, EW represents the amplitude of horizontal components and UD represents the amplitude of vertical component.

2.2. Theoretical H/V Spectral Ratios

Assuming that the fundamental-mode Rayleigh wave is dominant in the data set, the theoretical H/V spectral ratio is expressed as follows (Arai and Tokimatsu, 2004).

$$(H/V)_S(\omega) = \sqrt{\frac{P_{HR}(\omega)}{P_{VR}(\omega)}} \quad , \tag{2}$$

where P_{HR} and P_{VR} denotes the horizontal and vertical power of the observed surface waves in the frequency domain. Based on existing estimated 1D velocity structure models in Kathmandu Valley (Bhattarai et al., 2017; Dhakal et al., 2016), we constructed simplified velocity structure models that consists of two equivalent-thickness subsurface layers (Vs < 1000m/s) to estimate the depth of basement layer (Vs = 2200 m/s)

3. DATA

A research team of Oregon State University (OSU), the United States, installed 47 temporary seismic stations in collaboration with Department of Mines & Geology (DMG) from June 2015 to May 2016 to study the aftershock sequence in Nepal. There were three observation stations with three-component accelerometers inside the Kathmandu Valley (stations NAKRM, NANST & NABKT) and 16 aftershocks recorded during the observation period (4 ≤ ML ≤ 5.2; see Table 1). We retrieved the aftershock event data from the website of Incorporated Research Institution for Seismology (IRIS-DMC; https://ds.iris.edu/ds/nodes/dmc/forms/breqfast-request/),

Table 1. Earthquake event list from the IRIS Catalog.

No.	Time	yyyymmdd	Location	ML Local Catalog	Depth (km)
1	20:04	20150703	27.72S, 84.91E	4.5	3.36
2	15:29	20150706	27.94S, 85.69E	4.2	10
3	1:37	20150801	28.53S, 85.68E	4.0	10
4	13:02	20150814	27.57N, 86.07E	4.6	10
5	18:11	20150815	27.70N, 85.95E	4.7	10
6	22:23	20150817	27.90N, 86.13E	4.2	10
7	13:17	20150830	27.65N, 85.66E	4.5	10
8	14:52	20150916	27.59N, 86.19E	4.4	10
9	6:32	20150922	27.69S, 85.06E	4.2	7.48
10	10:54	20150929	27.77S, 85.82E	4.1	16.02
11	7:33	20151005	27.64S, 86.03E	4.5	10
12	12:02	20151006	27.77N, 86.15E	4.0	10
13	23:30	20151006	27.67N, 85.98E	4.3	14.04
14	4:15	20151119	27.85N, 85.68E	5	16.51
15	19:22	20160121	28.02N, 85.05E	4.5	19.01
16	16:20	20160205	27.84N, 85.25E	5.2	25.95

which were uploaded by International Federation of Digital Seismograph Networks (FDSN); http://www.fdsn.org/networks/detail/XQ_2015/). Continuous observations were conducted at the three sites and microtremor recordings are also available, so that we retrieved MHVSRs. A Japanese research team also conducted single-point microtremor observations with a three-component portable accelerometer at 11 sites inside the Kathmandu Valley five month after the mainshock (Yamada et al., 2017) and we used a part of the data.

4. RESULTS

4.1. EHVSRs and MHVSRs at three continuous observation stations

We used 16 aftershocks (Table 1) for calculations of EHVSRs. We retrieved 40.96 s time window from the S-wave onsets and calculated the EHVSRs at three stations NAKRM, NANST and NABKT for all recorded earthquakes. The result detects that stations NAKRM and NANST has a dominant peak at 0.59 and 0.29 Hz respectively in the low-frequency range and station NABKT shows a peak at 2.2 Hz in the high-frequency range (Figure 1).

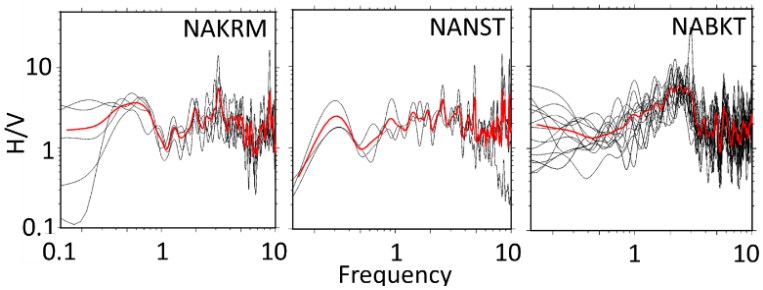

Figure 1. Derived EHVSRs from 16 aftershock events. Thin black curves denote the H/V spectral ratios from individual event and red curves denote the averaged ratios.

We also used continuous one-day microtremor data recorded at the same stations in different seasons. We divided the one-day microtremor data into 1-hour segments and derived MHVSRs together with noise Power Spectrum Density (PSD) to quantify the seismic background noise (McNamara and Buland, 2004). The MHVSR results indicated that stations NAKRM and NANST had a dominant peak at 0.6 and 0.27 Hz and station NABKT shows a peak at 2.2 Hz (Figure 2). This implies that accelerometers can be sometimes used for long-period microtremor survey as a substitute for long-period seismometers, when the amplitude microtremor is larger (especially in winter season). The comparisons between peak frequencies of EHVSRs and MHVSRs show linear relation to all three stations (Figure 3).

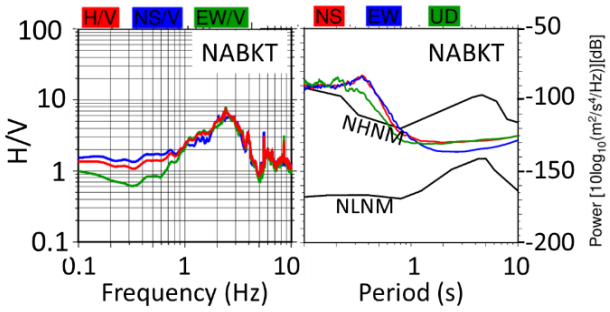

Figure 2. Derived MHVSR at NABKT station. This station shows peak frequency at 2.2 Hz and large PSD in short period range (< 1s).

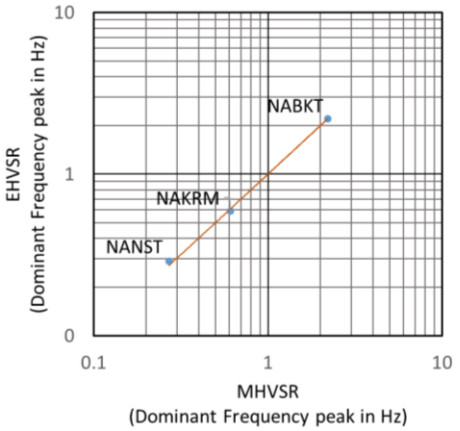

Figure 3. Comparison between dominant frequencies of EHVSR and MHVSR at stations NANST, NAKRM, NABKT.

4.2. MHVSRs at 11 temporary microtremor observation sites

We used single station microtremor survey data at 11 temporary stations inside the Kathmandu Valley (Yamada et al., 2017) and derived MHVSRs. The derived results showed dominant frequency peak range from 0.22 to 4.17 Hz (see an example in the Figure 4).

4.3. Estimated bedrock depth

The existing velocity models of the Kathmandu Valley; one simplified velocity structure model by Bhattarai et al., (2017) and another by Dhakal et al., (2016) were used to calculate the theoretical H/V spectral ratio. Comparing these theoretical H/V spectral ratio with the microtremor H/V peaks at three stations from OSU and 11 sites from J-RAPID microtremor study, we found the difference of bedrock depth between these two reference models (see Figures 5 and 6).

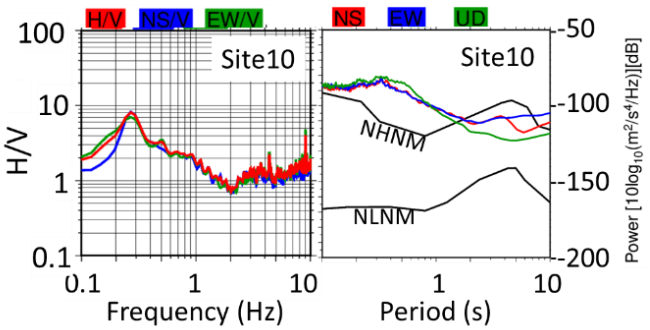

Figure 4. Derived MHVSR at Site10 station. The site shows the peak 0.28 Hz.

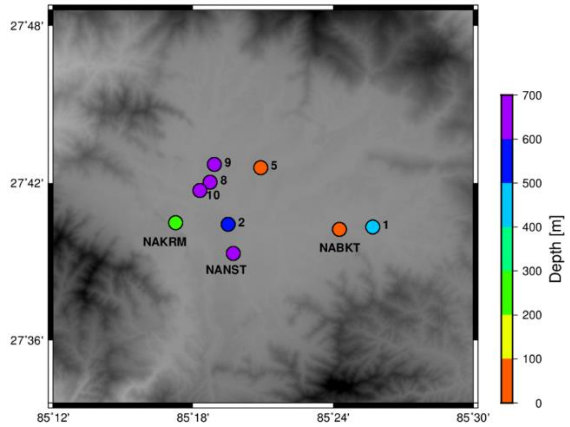

Figure 5. Map showing the depth at each station using the simplified model of Bhattarai et al., (2017).

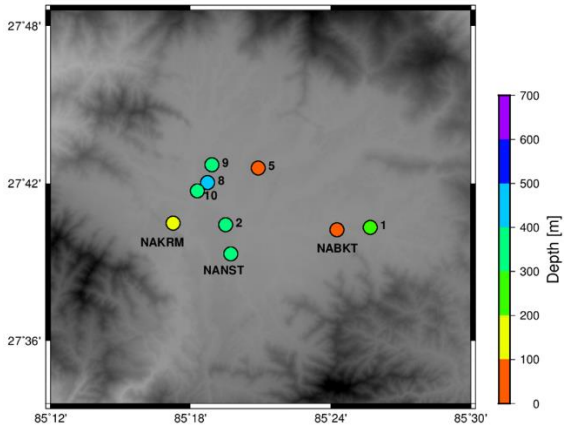

Figure 6. Map showing the depth at each station using the simplified model of Dhakal et al., (2016).

5. DISCUSSIONS

5.1. Seismic wave amplification inside Kathmandu Valley

To investigate the attenuation characteristics of high frequency seismic waves along the propagation direction and low-frequency amplification inside the basin, we selected three events; two aftershocks, Gorkha (4.6 ML) and Dolakha (4.5 ML) and one distant Afghanistan earthquake i.e. Hind-Kush (7.5 Mw). NANAT and NAKRM stations inside the Kathmandu Valley show high amplification in the lower frequency range for the distant event (epicentral distance of about 1600 km and station-to-station distance is almost 100 km). The dominant frequencies were 0.27 Hz at NANST and 0.57 Hz at NAKRM (Figure 7) corresponding well to those of the derived H/V ratios.

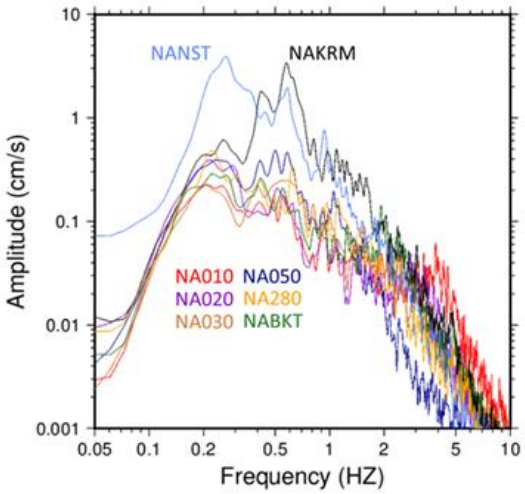

Figure 7. Observed Fourier spectra at five OSU stations. Two stations inside the basin (NAKRM, NANST) show large amplification in the low frequency range (0.1 to 1.0 Hz).

5.2. Seismic wave attenuation inside and outside of Kathmandu basin

Some researchers pointed out that high-frequency component seismic waves are significantly attenuated or scattered in the basin, while the low frequency components (< 0.1 to 1 Hz) are amplified. In order to prove whether the high-frequency component significantly attenuates or not, we selected two local earthquakes; Gorkha (mainshock area) and Dolakha (large aftershock area) and checked the attenuation of seismic waves along the propagation direction towards the Kathmandu basin. For this purpose, we estimated the theoretical amplitude spectra and compare them with observed spectra.

The following equation (Boore, 1983) was used to calculate the source effect.

$$S_a(f) = R_{\theta\emptyset} \; .PRTITN \; . \frac{\pi \; M_o}{\rho \; V_s^3} \; . \frac{f^2}{1 + \left(\frac{f}{f_c}\right)^2} \quad , \tag{3}$$

where $R_{\theta\emptyset}$ is the radiation pattern, *PRTITN* is the partitioning factor to convert the energy into two horizontal components, *Mo* is the seismic moment, ρ is the density around the source, *Vs* is the S-wave velocity around the source and *fc* is the corner frequency. To obtain seismic moment of two earthquakes, we used the Moment tensor inversion program developed by Yagi & Nishimura (2011). The program requires 1D seismic velocity structure model to compute Green's functions and we tested two structure models, a regional structure model by Pandey et al. (1995) and widely-used model by Jeffreys and Bullen (1958). Since the source depth of the earthquakes were not precisely determined and we searched the reliable source depths, changing the depth from 5 to 15 Km. The propagation path is expressed as,

$$P(f) = \frac{1}{r} \exp\left(\frac{-\pi f r}{Q(f) \; V_s}\right) \quad , \tag{4}$$

where r is the hypocentral distance (m), *Q(f)* is the quality factor which is equal to $100 \; f^{1.16}$ (Hazarika et al., 2013) & V_s is the S-wave velocity.

Site effect *G(f)* is set as 2.0 for the hard rock site.

Figure 8 compares observed and theoretical acceleration spectra for Dolakha event. Here we can clearly see that the observed spectra are quite similar to the theoretical ones, when we assumed corner frequency at around 4 Hz. This estimation well correlate with the value proposed in the past research (Timsina et al., 2018). The stations NANST & NAKRM show large amplifications in the lower frequency range, but we cannot identify any decay of high frequency motions. This clearly shows that the thick sedimentary layers only amplify the input motion from 0.1 Hz to 1.0 Hz and do not significantly attenuate seismic ground motions.

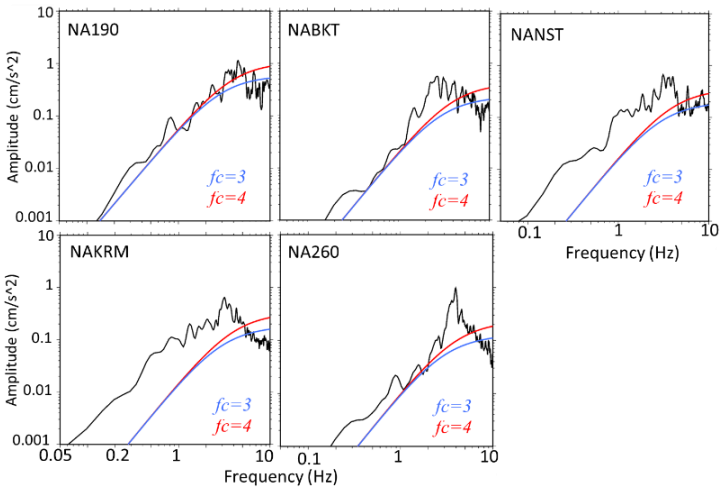

Figure 8. Comparisons between observed and theoretical acceleration spectra for Dolakha event. Stations NANST and NAKRM inside the Kathmandu Valley shows large amplification in the low frequency range, while there are no significant differences in the higher frequencies. Blue and red traces indicate theoretical spectra for different corner frequencies (*fc*=3Hz and 4Hz, respectively).

6. CONCLUSIONS

The main findings from this study are as follows:

i. Estimated dominant peak frequencies from EHVSRs and MHVSRs corresponds to each other in the Kathmandu Valley. We identified the peaks at NANST (0.32 Hz), at which the thick sedimentary layer could exists.
ii. Theoretical H/V ratios show that the sedimentary layer had a thickness ranges from 42 to 700 m in the study sites.
iii. The velocity spectra derived from Afghanistan event and the amplitude spectra derived from Dolakha and Gorkha event shows that large seismic amplifications were observed in the lower frequency range at basin stations (0.1-1.0 Hz).
iv. The spectra of local event showed that the attenuation of high-frequency seismic waves are not significantly attenuated in the Kathmandu basin.

7. RECOMMENDATION

The accurate estimation of bedrock depth using single station microtremor data is difficult. However, the data showed the spatial variation of bedrock depth in the Kathmandu Valley. The combined use of H/V and other approach, such as microtremor array exploration, receiver function analysis and gravity survey would help to understand detailed 3D basin structure model.

ACKNOWLEDGEMENTS

I would like to express my sincere gratitude to the supervisors Dr. Toshiaki YOKOI and Dr. Takumi HAYASHIDA for their tremendous support, valuable suggestion and instruction during my study. I would like to extend my gratitude to DMG, JICA, IISEE and GRIPS for the opportunity to study this course.

REFERENCES

Arai, H., and Tokimatsu, K., 2004, BSSA, Vol. 94, No. 1, 53-63.
Bhattarai, M. et al.,2015, Seismological Research Letters, Vol. 86: 1540-1548.
Bhattarai, M. et al.,2017, Proceedings of the 13th Annual Meeting of JAEE, P4-32.
Boore, D.M., 1983, Bull. Seism. Soc. Am. 73, 1865-1894.
Dhakal, Y. P. et al., 2016, Earth, Planets and Space, DOI: 10.1186/s40623-016-0432-2.
Hazarika, P. et al., 2013, Geophys. J. Int. (2013) 195, doi: 10.1093/gji/ggt241, pp 544-557.
Jeffreys, H., and Bullen, K. E., 1958, Office of the British Association, Burlington House, London.
Kanai, K. and Tanaka, T., 1954, On Bull. Earthquake Res. Inst. 32,199–209.
McNamara, D.E. and Buland R.P., 2004, Bulletin of Seismological Society of America, Vol.94.
Moribayashi, S., and Maruo, Y., 1980, Journal of Japan Society of Engineering Geology 21, 30-37.
Nakamura, Y., 1988, Quality Report on Railroad Research, Vol. 4, Railway Technical Research Institute,18–27 (in Japanese).
Pandey, M.R. et al., 1995, Geophys. Res. Lett., 22, 751–754.
Takai, N. et al., Earth Planets Space, DOI:10.1186/ s40623-016-0383-7.
Timsina, C. et al., 2018, the 12th General Assembly of the Asian Seismological Commission.
Yagi, Y., and Nishimura, N., 2011, Bull. of IISEE 45, 133–138.
Yamada, M. et al., 2016, Earth, Planets and Space, DOI: 10.1186/s40623-016-0483-4.
Website: IRIS, https://ds.iris.edu/ds/nodes/dmc/forms/breqfast-request/
Website: FDSN, http://www.fdsn.org/networks/detail/XQ_2015/